This document is the accepted manuscript version of the following article:
Mohn, J., Gutjahr, W., Toyoda, S., Harris, E., Ibraim, E., Geilmann, H., … Brand, W. A. (2016). Reassessment of the NH4NO3 thermal decomposition technique for calibration of the N2O isotopic composition. Rapid Communications in Mass Spectrometry, 30(23), 2487-2496. https://doi.org/10.1002/rcm.7736

Reassessment of the NH_4NO_3 thermal decomposition technique for calibration of the N_2O isotopic composition

Joachim Mohn[1,*], Wilhelm Gutjahr[1], Sakae Toyoda[2], Eliza Harris[1], Erkan Ibraim[1], Heike Geilmann[3], Patrick Schleppi[4], Thomas Kuhn[5], Moritz F. Lehmann[5], Charlotte Decock[6], Roland A. Werner[7], Naohiro Yoshida[2,8] and Willi A. Brand[3]

[1] Laboratory for Air Pollution & Environmental Technology, Empa, Swiss Federal Laboratories for Materials Science and Technology, Überlandstr. 129, CH-8600 Dübendorf, Switzerland

[2] Department of Chemical Science and Engineering, Tokyo Institute of Technology, 4259 Nagatsuta, Midori-ku, Yokohama 226-8502, Japan

[3] Stable Isotope Laboratory (IsoLab), Max-Planck-Institute for Biogeochemistry (MPI-BGC), Hans-Knöll-Str. 10, D-07745 Jena, Germany

[4] Forest Soils and Biogeochemistry, WSL, Zürcherstrasse 111, CH-8903 Birmensdorf, Switzerland

[5] Biogeochemistry, University of Basel, Bernoullistrasse 30, CH-4056 Basel, Switzerland

[6] Sustainable Agroecosystems, ETH Zürich, Tannenstrasse 1, CH-8092 Zürich, Switzerland

[7] Institute of Agricultural Sciences, ETH Zürich, Universitätstrasse 2, CH-8092 Zürich, Switzerland

[8] Earth-Life Science Institute, Tokyo Institute of Technology, 2-12-1 Ookayama, Meguro-ku, Tokyo 152-8550, Japan

Correspondence to: J. Mohn, Laboratory for Air Pollution & Environmental Technology, Empa, Überlandstr. 129, CH-8600 Dübendorf, Switzerland. tel. +41 58 765 4687, fax +41 58 765 2211, E-mail: joachim.mohn@empa.ch

Key words: nitrous oxide, isotopic composition, site-preference, NH_4NO_3 thermal decomposition, isotope fractionation

Abstract

RATIONALE: In the last few years, the study of N_2O site-specific nitrogen isotope composition has been established as a powerful technique to disentangle N_2O emission pathways. This trend has been accelerated by significant analytical progress in the field of isotope–ratio mass–spectrometry (IRMS) and more recently quantum cascade laser absorption spectroscopy (QCLAS).

METHODS: The ammonium nitrate (NH_4NO_3) decomposition technique provides a strategy to scale the ^{15}N site-specific ($SP \equiv \delta^{15}N^{\alpha} - \delta^{15}N^{\beta}$) and bulk ($\delta^{15}N^{bulk} = (\delta^{15}N^{\alpha} + \delta^{15}N^{\beta}) / 2$) isotopic composition of N_2O against the international standard for the $^{15}N/^{14}N$ isotope ratio (AIR-N_2). Within the current project ^{15}N fractionation effects during thermal decomposition of NH_4NO_3 on the N_2O site preference were studied using static and dynamic decomposition techniques.

RESULTS: The validity of the NH_4NO_3 decomposition technique to link NH_4^+ and NO_3^- moiety-specific $\delta^{15}N$ analysis by IRMS to site-specific nitrogen isotopic composition of N_2O was confirmed. However, the accuracy of this approach for calibration of $\delta^{15}N^{\alpha}$ and $\delta^{15}N^{\beta}$ was found to be limited by non-quantitative NH_4NO_3 decomposition in combination with substantially different isotope enrichment factors for the conversion of the NO_3^- or NH_4^+ nitrogen atom into the α or β position of the N_2O molecule.

CONCLUSIONS: The study reveals that the completeness and reproducibility of the NH_4NO_3 decomposition reaction currently confines the anchoring of N_2O site specific isotopic composition to the international isotope ratio scale AIR-N_2. The authors suggest to establish a set of N_2O isotope reference materials with appropriate site-specific isotopic composition, as community standards, to improve inter-laboratory compatibility.

INTRODUCTION

Important information on the transformation processes of the potent greenhouse gas and ozone depleting substance nitrous oxide (N_2O) is acquired by analysing its ^{15}N site-specific and bulk isotopic composition[1, 2]. In the last two decades, research involving N_2O isotopic analysis was stimulated by continuing analytical progress in IRMS and more recently quantum cascade laser based absorption spectroscopy (QCLAS). The mass spectrometric analytical technique for the analysis of the intramolecular ^{15}N distribution within the linear asymmetric N_2O molecule was accomplished first by Toyoda and Yoshida[3] and by Brenninkmeijer and Röckmann[4]. Since its first realization at Empa in 2008[5], QCLAS and cavity ring-down spectroscopy (CRDS) have been established as independent analytical techniques offering high selectivity for the N_2O isotopic species ($^{14}N^{15}N^{16}O$, $^{15}N^{14}N^{16}O$, $^{14}N^{14}N^{16}O$, $^{14}N^{14}N^{18}O$)[6] and the capability for real-time analysis[7-9]. Throughout the manuscript the terms “isotopomer”, for molecular species having the same number of each isotopic atom but differing in their positions ($^{14}N^{15}N^{16}O$, $^{15}N^{14}N^{16}O$) and “isotopologue”, for molecular species that differ in the isotopic composition ($^{15}N^{14}N^{16}O$, $^{14}N^{14}N^{16}O$, $^{14}N^{14}N^{18}O$), are used. To specify the location of ^{15}N substitution in the N_2O molecule, the central and terminal nitrogen atom are designated as α and β position, respectively[3]. The umbrella term "isotopocules" is applied to refer to both isotopomers and isotopologues[10]. Irrespective of the achieved analytical progress, however, the compatibility between laboratories for the N_2O isotopic composition is still limited to several δ -per mil units, due to the restricted availability of suitable reference materials[11].

The synthesis of N_2O by thermal decomposition of isotopically characterised ammonium nitrate (NH_4NO_3) has been suggested as an approach to link the position-dependent nitrogen isotopic composition of N_2O relative to the international standard for the $^{15}N/^{14}N$ isotope ratio, AIR-N_2[3]. The basic concept of this technique is that the nitrogen atom at the central (α) position of product N_2O originates from the NO_3^- ion, while the end (β) nitrogen comes from the NH_4^+

ion[3, 12]. The initial inconsistency with a second approach, the addition of small amounts of $^{15}N_2O$ to a N_2O reference gas and tracking changes in the relative ion current species with mass 30, 31, 44, 45, and 46[13], was resolved by Westley et al.[14] and Griffith et al.[15] . They advocate inter-calibration of N_2O isotope measurement results with Tokyo Institute of Technology as the most efficient and reliable method for standardization and claim that isotope fractionation effects during NH_4NO_3 decomposition are small and symmetrically distributed, which is an essential requirement for the validity of this approach.

In the presented study we reassessed the validity of the NH_4NO_3 decomposition technique to scale the position-dependent nitrogen isotopic composition of N_2O to the international isotope ratio standard AIR-N_2. In detail the following approach was applied: (1) NH_4NO_3 salts with different isotopic composition were prepared and analysed by IRMS; (2) the same NH_4NO_3 salts were decomposed and isotope fractionation effects for $\delta^{15}N^{\alpha}$, $\delta^{15}N^{\beta}$ and $\delta^{18}O$ were studied in flow-through and static thermal decomposition experiments by QCLAS; (3) in addition, $\delta^{15}N^{bulk}$ and $\delta^{18}O$ of N_2O, produced by thermal decomposition, were analysed by IRMS relative to AIR-N_2 and Vienna Standard Mean Ocean Water (VSMOW).

EXPERIMENTAL

Preparation of NH_4NO_3 salts

Four NH_4NO_3 salts (P1 – P4) with different isotopic composition were prepared by gravimetric mixing of NH_4NO_3 (≥ 98 %, Carl Roth GmbH, Karlsruhe, Germany) with isotopically pure (98 atom % ^{15}N) $^{15}NH_4NO_3$ (Sigma-Aldrich Chemie GmbH, Buchs, Switzerland) and (≥ 98 %, 99.9 atom % ^{14}N) $^{14}NH_4{}^{14}NO_3$ (Cambridge Isotope Laboratories Inc., Tewksbury, USA). The prepared NH_4NO_3 mixtures were recrystallized in 20 mL deionized water and dried overnight at 393 K. The isotopic homogeneity of the recrystallized salts was assessed by triplicate thermal decomposition and subsequent QCLAS analysis. The isotopic composition of N_2O ($\delta^{15}N^{\alpha}$,

$\delta^{15}N^{\beta}$ and $\delta^{18}O$) from individual decomposition experiments coincided within the analytical precision of 0.1 - 0.2 ‰.

Isotopic analysis of NH_4NO_3 by IRMS

The four NH_4NO_3 salts were analysed by four different IRMS laboratories (Laboratory 1A and 1B, 2 and 3) for $\delta^{15}N\text{-}NO_3^-$ and $\delta^{15}N\text{-}NH_4NO_3$ using their in-house analytical techniques. $\delta^{15}N\text{-}NH_4^+$ was calculated from $\delta^{15}N\text{-}NH_4NO_3$ and $\delta^{15}N\text{-}NO_3^-$.

Laboratory 1A: $\delta^{15}N$ and $\delta^{18}O$ in the NO_3^- moieties were determined after conversion of NO_3^- to N_2O by the bacterial denitrifier assay[16, 17]. For each of the four NH_4NO_3 salts (P1 - P4), four replicate samples were prepared for the denitrifier method, along with the nitrate calibration standards USGS32 (KNO_3, $\delta^{15}N^{bulk}$ = 180 ± 1 ‰, $\delta^{18}O$ = 25.7 ± 0.4 ‰), USGS34 (KNO_3, $\delta^{15}N^{bulk}$ = -1.8 ± 0.2 ‰, $\delta^{18}O$ = -27.9 ± 0.6 ‰) and USGS35 ($NaNO_3$, $\delta^{15}N^{bulk}$ = 2.7 ± 0.2 ‰, $\delta^{18}O$ = 57.5 ± 0.6 ‰), supplied by NIST (National Institute of Standards and Technology, Gaithersburg, MD). Additional standards were included in the batch to monitor and correct for instrumental drift and linearity. Isotope ratios of $^{15}N/^{14}N$ and $^{18}O/^{16}O$ in N_2O were measured using a ThermoFinnigan GasBench + PreCon trace gas concentration system interfaced to a ThermoScientific Delta V Plus isotope-ratio mass spectrometer (Bremen, Germany). Gas samples were purged from vials through a double-needle sampler into a helium carrier stream (25 mL min^{-1}). CO_2 is removed from the sample by passing through an Ascarite scrubber. N_2O is trapped and concentrated in two cryo-traps at 77 K (liquid N_2) operated in series. It is released from the traps in the helium carrier gas by warming and subsequently passed to the mass spectrometer via an Agilent GS-Q capillary column (30 m x 0.32 mm, 313 K, 1.0 mL min^{-1}, Agilent Technologies Inc., Santa Clara, USA). A reference N_2O peak is used to calculate provisional isotope ratios of the sample N_2O peak. Final corrected isotope values are calculated based on the provisional isotope ratios and the known isotope ratios of the nitrate calibration

standards. The in-house limit of quantitation was determined to be 2 µM NO_3^- in water, the repeatability for $\delta^{15}N$ and $\delta^{18}O$ of N_2O from NO_3^- by bacterial denitrification was 0.4 ‰ for $\delta^{15}N$ and 0.5 ‰ for $\delta^{18}O$, respectively.

Laboratory 1B: The measurement of $\delta^{15}N$-NH_4NO_3 values of P1 – P4 was performed using a Flash EA 1112 Series elemental analyzer (Thermo Italy, former CE Instruments, Rhodano, Italy) coupled to a Finnigan MAT Delta^{plus}XP isotope–ratio mass–spectrometer (Finnigan MAT, Bremen, Germany) via a 6-port valve[18] and a ConFlo III (Finnigan MAT, Bremen, Germany)[19]. The positioning of samples, blanks and (laboratory) standards in a measurement sequence followed the Identical Treatment principle described by Werner and Brand[20]. Post-run off-line calculations like blank-, offset- and possibly drift-corrections and a normalization for assigning the final $\delta^{15}N$-values on the AIR-N_2 scale were performed according to Werner and Brand[20]. Calibration of laboratory standards was periodically done by comparison of the laboratory standards (acetanilide, caffeine, tyrosine) to the corresponding international reference materials (IAEA-N-1: $(NH_4)_2SO_4$, $\delta^{15}N^{bulk}$ = 0.4 ± 0.2 ‰, IAEA-N-2: $(NH_4)_2SO_4$, $\delta^{15}N^{bulk}$ = 20.3 ± 0.2 ‰, IAEA-NO-3: KNO_3, $\delta^{15}N^{bulk}$ = 4.7 ± 0.2 ‰) provided by the IAEA (Vienna, Austria). The repeatability (several years) of our quality control standard (tyrosine) was 0.15 ‰ or better for $\delta^{15}N$.

Laboratory 2: Analyses of the $\delta^{15}N$-NH_4NO_3 of salts P1 – P4 were performed by elemental analyser–isotope–ratio mass–spectrometry (EA-IRMS) using an INTEGRA 2 instrument (Sercon Ltd., Crewe, UK). Each salt has been measured in five replicates. In view of the ammonium and nitrate moieties, which chemically constitute the four salts, and the expected span in $\delta^{15}N$ the following five isotopic reference materials have been measured in replicates at the beginning, in the middle, and at the end of the analytical sequence: IAEA-N-1 ($(NH_4)_2SO_4$, $\delta^{15}N^{bulk}$ = 0.4 ± 0.2 ‰) and USGS26 ($(NH_4)_2SO_4$, $\delta^{15}N^{bulk}$ = 53.7 ± 0.4 ‰), IAEA-

NO-3 (KNO_3, $\delta^{15}N^{bulk}$ = 4.7 ± 0.2 ‰) and USGS32 (KNO_3, $\delta^{15}N^{bulk}$ = 180 ± 1 ‰), and RSIL-N7373 (Reston Stable Isotope Laboratory, U.S. Geological Survey, Reston, USA, $NaNO_2$, $\delta^{15}N^{bulk}$ = -79.6 ‰)[18]. These reference materials were used to check and correct for instrumental drift and for normalization to the AIR-N_2 scale. In order to avoid potential amount linearity effects, the analyzed quantities of the reference materials and salt samples were adjusted to contain (virtually) equal amounts of nitrogen. The repeatability for reference materials IAEA-N-1, USGS26, IAEA-NO-3, and USGS32 was ≤ 0.3 ‰ (1 σ, n = 10). Reference material RSIL-N7373, which was specifically included in the analyses due to its very low $\delta^{15}N$ value of -79.6 ‰, exhibited a repeatability of 0.4 ‰ (1 σ, n = 10).

For analyses of the $\delta^{15}N$ of the nitrate-moiety ($\delta^{15}N$-NO_3^-) of P1 – P4, the salts as well as blanks and four international isotopic reference materials (IAEA-NO-3, USGS32, RSIL-N23[21]: Reston Stable Isotope Laboratory, $NaNO_2$, $\delta^{15}N^{bulk}$ = 3.7 ‰, RSIL-N7373) were prepared in replicates (P1 - P4: n = 5, reference materials: n = 4, respectively) using the "denitrifier method"[16, 17] , modified according to McIlvin and Casciotti (2011)[22]. This method employs the denitrifying bacterium *Pseudomonas aureofaciens* (ATTC no. 13985), which lacks the N_2O reductase enzyme and quantitatively converts sample-derived NO_3^- to N_2O. The four reference materials were chosen with regard to the principle of identical treatment[20] and covering a wide-enough range in $\delta^{15}N$ for isotopic calibration (RSIL-N7373: -79.6 ‰; USGS32: 180 ± 1 ‰). Isotope analysis of the obtained N_2O was performed on an instrument consisting of an N_2O purification and purge-and-trap system designed after McIlvin and Casciotti (2010)[23], which is coupled to a Delta V Plus isotope–ratio mass–spectrometer (Thermo Fisher Scientific, Bremen, Germany). The four reference materials were used to check for potential instrumental drift and normalization to the AIR-N_2 scale. The repeatability (1σ) of $\delta^{15}N$-NO_3^- for the replicates of the reference materials (n = 4) and salts (n = 5) was ≤ 0.2 ‰.

Laboratory 3: $\delta^{15}N\text{-}NO_3^-$ and $\delta^{15}N\text{-}NH_4NO_3$ analysis of individual salts P1 – P4 was performed in triplicate or quadruplicate as described by P. Schleppi et al.[24]. The applied technique also has the potential to determined $\delta^{15}N\text{-}NH_4^+$ values, which were not used for data interpretation, due to variable fractionation effects. Rather, $\delta^{15}N\text{-}NH_4^+$ was calculated from $\delta^{15}N\text{-}NH_4NO_3$ and $\delta^{15}N\text{-}NO_3^-$. For $\delta^{15}N\text{-}NO_3^-$ analysis, around 180 µL of a 32 µmol L^{-1} aqueous NH_4NO_3 solution were supplemented with 40 mL of 0.7 mol L^{-1} KCl solution (p.a., Sigma-Alrich Chemie GmbH, Switzerland) in a 100 mL polyethylene flasks. NH_4^+ was removed by addition of 1.5 g L^{-1} MgO (Sigma-Alrich Chemie GmbH, Switzerland) over 5 days on a mechanical shaker. Thereafter, a 12 x 5 mm calcinated glass filter cut from round filters GF/F; (Whatman plc, Little Chalfont, UK), drenched with 30 µL of 2 mol L^{-1} citric acid (Sigma-Alrich Chemie GmbH, Switzerland) and sealed with a PTFE band by forming an envelope (Angst + Pfister, Zurich, Switzerland) was added. 0.4 g Devarda's alloy (Sigma-Alrich Chemie GmbH, Switzerland) were added to initiate NO_3^- reduction to NH_4^+ and the solution was stirred for one week on a horizontal shaker. Thereafter, the filter was dried in a desiccator for 45 minutes, the PTFE membrane removed and the glass filter packed in a tin (Sn) capsule for subsequent IRMS analysis. For $\delta^{15}N\text{-}NH_4NO_3$ analysis, 30 µL of aqueous 0.2 mol L^{-1} NH_4NO_3 solution were pipetted directly onto glass filters, sealed with a PTFE band and dried for 45 minutes in a desiccator. Then, the PTFE band was removed and the glass filters packed in Sn capsules for IRMS analysis. Blank values for $\delta^{15}N\text{-}NH_4NO_3$ and $\delta^{15}N\text{-}NO_3$ analysis were determined with 0.7 mol L^{-1} KCl solution without NH_4NO_3 addition. After conversion to N_2 with an elemental analyser (Euro EA3000, Eurovector Srl, Milano, Italy), $^{15}N/^{14}N$ isotope ratios were determined by IRMS (DeltaV Advantage, Thermo Fisher Scientific Inc., Germany). Relative differences of isotope ratios ($\delta^{15}N$) to the international isotope ratio scale AIR-N_2, were determined by analysis of NIST Standard 1547 (peach leaves 996) ($\delta^{15}N^{bulk}$ = 1.969 ‰). All results were corrected for the nitrogen content and $\delta^{15}N$ values observed for the corresponding blanks.

Thermal decomposition of NH_4NO_3 – static method

For this method 1.3 g (16.2 mmol) of NH_4NO_3 (P1 – P4) were weighed into quartz-glass round-bottom flasks with break-seal (150 mL, Duran glass, Glasbläserei Willi Möller AG, Zürich, Switzerland), evacuated (< 10^{-1} mbar) and flame-sealed. In addition for P1 smaller quartz glass ampoules with break-seal (4.4 mL, Duran glass, Glasbläserei Willi Möller AG, Zürich, Switzerland) were used for the initial isotope fractionation experiments filled with 60 – 80 mg (0.7 – 1.0 mmol) of NH_4NO_3. The sealed flasks or ampoules were placed in a circulating air oven (SalvisLab, Rotkreuz, Switzerland) and heated by 1.0 K min^{-1} up to 543 K. For the isotope fractionation experiments (P1) the hold time at 543 K was set to vary between 1 and 24 hours in order to vary the yield of the thermal decomposition reaction. For the reassessment of the NH_4NO_3 decomposition reaction (P1-P4), a hold time of 24 hours was used to achieve maximum reaction yield. After the defined hold time quartz glass containers were removed from the oven and allowed to cool to room temperature. This is slightly different from the procedure applied by Toyoda, where the flasks remain in the oven after decomposition and are allowed to cool down more slowly (Sakae Toyoda, personal communications). Afterwards, the N_2O product gas was purified on a vacuum manifold by multiple cryogenic distillations. Reaction by-products and side-products (e.g. H_2O, HNO_3, NH_3) were trapped at 195 K (dry ice / ethanol bath) and N_2O at 77 K (liquid N_2), while N_2 and O_2 were removed by evacuation with an oil sealed rotary vane pump (RV3, Edwards Ltd., Crawley, UK). The N_2O yield of the decomposition reaction was calculated based on the mass of the NH_4NO_3 substrate and the volume of the product gas N_2O calculated from the inner volume of the gas line normalized for pressure (LEO3 Manometer, Keller AG, Winterthur, Switzerland) and temperature (GMH 3750 and GTF601, GHM-Greisinger, Regenstauf, Germany). The uncertainty of the yield was estimated using the laws of error propagation.

The yield of N_2 and O_2 was estimated from the pressure decrease after evacuation of the condensable gases at 77 K (liquid N_2). The purified N_2O product gas was filled in 50 mL stainless steel cylinders (SS-4CS-TW-50, Swagelok AG, Niederrohrdorf, Switzerland) and analysed by IRMS at Max-Planck-Institute for Biogeochemistry (MPI-BGC) as described in the following. For site-specific N_2O isotopic analysis by QCLAS the N_2O product gas was diluted in a two-step procedure with high–purity synthetic air (99.999 %, 20.5 % O_2 in N_2) to a target N_2O mole fraction of 90 ppm (10^{-6} moles per mole of dry air). First a static dilution was performed in triplicate, where 3 mL of pure N_2O at 3000 to 5000 hPa were purged with synthetic air into a 6 L stainless steel cylinder (S6L Aerosphere, Labcommerce Inc., San Jose, USA) via a ten-port 2-position valve (EH2C10WEPH equipped with 3 mL sample loop, Valco Instruments Inc., Schenkon, Switzerland) to a final pressure of 2800 hPa. Secondly, a dynamic dilution was performed (mass flow controller, Vögtlin Instruments AG, Aesch, Switzerland) with synthetic air prior to analysis by QCLAS.

Thermal decomposition of NH_4NO_3 – dynamic method

Around 70 mg (0.9 mmol) of ammonium nitrate (P1) were placed into a quartz glass tube (12 mm outer diameter (OD), length 20 cm, Duran glass, Willi Möller AG, Zürich, Switzerland), which was purged with 10 mL min^{-1} high purity nitrogen gas (99.999 %, Messer Schweiz AG, Lenzburg, Switzerland). The temperature of the tube was increased by 1.5 K min^{-1} to a final temperature of 543 K. Downstream of the heated glass tube the reaction gas was diluted with 250 mL min^{-1} high purity synthetic air (99.999 %, 20.5 % O_2 in N_2) and transferred through a heated PTFE line (453 K, Winkler GmbH, Heidelberg, Germany) to an FTIR spectrometer (CX-4000, Gasmet Technologies Oy, Helsinki, Finland). N_2O mixing ratios and reaction by-products (H_2O, NH_3, NO, NO_2, HNO_3) were quantified in real-time by Fourier Transform Infrared Spectroscopy (FTIR)[25, 26]. Downstream of the FTIR spectrometer the process gas was dynamically diluted to a constant N_2O mole fraction of 90 ppm. The dilution ratio was

calculated on-line based on FTIR results and used to automatically (LabVIEW, National Instruments Switzerland Corp., Ennetbaden, Switzerland) set the dilution flow of synthetic air (mass flow controller, Vögtlin Instruments AG, Aesch, Switzerland)[27]. Thereafter, the N_2O isotopic composition was analysed by QCLAS (Aerodyne Research Inc., Billerica, USA), as described below[5].

Analysis of N_2O site-specific isotopic composition by QCLAS (Empa)

Isotopic analysis of N_2O produced by static or dynamic thermal NH_4NO_3 decomposition was performed by QCLAS. The employed laser spectrometer (Aerodyne Research Inc., Billerica, USA) was previously described by our laboratory in a number of studies[6, 8, 28, 29]. It includes a continuous wave quantum cascade laser source emitting at 2203 cm^{-1} (Alpes Lasers, St Blaise, Switzerland), which enables the simultaneous quantification of the four most abundant N_2O isotopic species ($^{14}N^{14}N^{16}O$, $^{15}N^{14}N^{16}O$, $^{14}N^{15}N^{16}O$, and $^{14}N^{14}N^{18}O$). The spectrometer was operated in a flow-through mode (50 mL min^{-1}) with a gas cell pressure and temperature of 25 hPa and 293 K, respectively. Ratios of N_2O isotopologues ($^{15}N^{14}N^{16}O/^{14}N^{14}N^{16}O$, $^{14}N^{15}N^{16}O/^{14}N^{14}N^{16}O$, $^{14}N^{14}N^{18}O/^{14}N^{14}N^{16}O$) were analysed at 1 Hz temporal resolution with a precision of < 0.6 ‰; with 450 s spectral averaging the spectrometer enables high precision analysis (<0.05 ‰, Allan precision[30]) of isotope ratios. The spectroscopically determined isotope ratios were related to the international isotope ratio scales (AIR-N_2 for $^{15}N/^{14}N$, VSMOW for $^{18}O/^{16}O$) through analysis of calibration gases CG1 (CG1-1: $\delta^{15}N^{\alpha}$ = 2.06 ± 0.05 ‰. $\delta^{15}N^{\beta}$ = 1.98 ± 0.20 ‰, $\delta^{18}O$ = 36.12 ± 0.3 ‰; CG1-2: $\delta^{15}N^{\alpha}$ = -0.13 ± 0.28 ‰. $\delta^{15}N^{\beta}$ = 1.35 ± 0.29 ‰, $\delta^{18}O$ = 38.46 ± 0.15 ‰) and CG2 ($\delta^{15}N^{\alpha}$ = -82.14 ± 0.49 ‰. $\delta^{15}N^{\beta}$ = -78.02 ± 0.52 ‰, $\delta^{18}O$ = 21.64 ± 0.12‰) before and after every experiment. The isotopic composition of the calibration gases has been previously analysed by Tokyo Institute of Technology using their analytical technique as a link to the international scales.

The uncertainty in delta values, $\delta^{15}N^{\alpha}$, $\delta^{15}N^{\beta}$, $\delta^{18}O$, $\delta^{15}N^{bulk}$ and SP, of N_2O analysed by QCLAS was calculated from the standard deviation for repeated measurements by QCLAS and the standard deviation of calibration gases provided by Tokyo Institute of Technology using the laws of error propagation.

Analysis of $\delta^{15}N^{bulk}$ by IRMS (MPI-BGC)

Pure N_2O was introduced with a six port 2-position valve (Valco Instruments Inc., Schenkon, Switzerland) equipped with a 250 µl loop at 3000 – 4000 hPa. The valve was inserted into the transfer line between the oxidation and the reduction reactor of an EA 1110 CHN combustion analyser (CE Instruments Ltd, Wigan, UK). Isotopic analysis was made by coupling the EA effluent via a ConFlo III interface (Finnigan MAT, Bremen, Germany) to a Delta plus isotope–ratio mass–spectrometer (Thermo-Fisher, Bremen, Germany). Complete conversion of N_2O to N_2 in the reduction reactor was checked by monitoring the mass-to-charge ratio (*m/z*) 44 after N_2O injection. No appreciable signal was found, except small amounts of NO_2 on *m/z* 46, indicating formation of this gas on the filament when N_2 enters the ion source, which does not interfere with the measurement. IAEA-N1 (ammonium sulphate) with an assigned value of 0.43 ‰ on the AIR-N_2 scale was used as the scale anchor. Additionally, an in-house working reference material "Ali-J3", an acetanilide sample calibrated with IAEA-N1 was used. We refer to these substances as 'combustible reference materials'. CO_2 and humidity from reference material combustion was removed using an Ascarite trap (NaOH on pumice) and $Mg(ClO_4)_2$ mounted in front of the EA-GC[18]. The measurements were made by injecting the combustible reference, followed by a number of N_2O injections, and converting the measured isotopic distance to the AIR-N_2 scale.

Analysis of $\delta^{18}O$ by IRMS (MPI-BGC)

Plain air and pure N_2O were injected via a 1 mL loop into the TC/EA high temperature conversion elemental analyser (CE Instruments Ltd, Wigan, UK) to produce CO from both. The reaction gases (N_2 and CO) were fully baseline-separated on the gas chromatograph and analysed on-line via a ConFlo III interface and Delta^{plus}XL isotope–ratio mass–spectrometer (Thermo-Fisher, Bremen, Germany). Compressed clean-sector, ultra-dry Jena air with $\delta^{18}O$ (VSMOW) = 23.88 ‰ was used as scale anchor[31].

RESULTS AND DISCUSSION

Isotope fractionation effects during thermal decomposition of NH_4NO_3 – static method

Figure 1 presents the site-specific isotopic composition of the accumulated product N_2O generated by thermal decomposition of NH_4NO_3 salt P1. $\delta^{15}N^{\alpha}$, $\delta^{15}N^{\beta}$ and $\delta^{18}O$ offer a distinct dependence on the reaction yield, which increases with increasing hold time at constant decomposition temperature (543 K), and reaches 91.2 ± 2.3 to 93.5 ± 2.4 % after 24 hours. A further increase in hold time to 68 hours did not significantly affect N_2O production (90.5 ± 2.5 %). Plotting relative differences of isotope ratios of the accumulated product N_2O versus -f ln f / (1-f) displays a linear relationship (Figure 1), with f being the fraction of the remaining substrate. The regression line is defined as (Eqn. (1))[32]:

$$\delta_{N_2\,O} = \delta_{NH_4\,NO_3} - \varepsilon \times \frac{f \times lnf}{(1-f)} \quad (1)$$

where the slope ε is the isotope enrichment factor of the reaction, assuming validity of the Rayleigh isotope fractionation model (e.g. unidirectionality, single-step reaction and constant ε). In particular the assumption of single-step reaction and isotope mass balance, which implies the absence of side reactions (or the isotopic characterisation of side-products) is only a first approximation, as discussed below and in the following sections.

The observed isotope enrichment factors indicate a pronounced fractionation for the conversion of the NH_4^+ nitrogen atom to the end (β) position of the N_2O molecule ($\varepsilon_{NH4\text{-}15N\beta}$ = -18.88 ± 0.94 ‰), while isotope fractionation effects are considerably less pronounced for the transformation of the NO_3^- nitrogen atom to the middle (α) position of the N_2O molecule ($\varepsilon_{NO3\text{-}15N\alpha}$ = -4.23 ± 0.55 ‰) and for the O atom ($\varepsilon_{NO3\text{-}18O}$ = 1.77 ± 0.43 ‰).

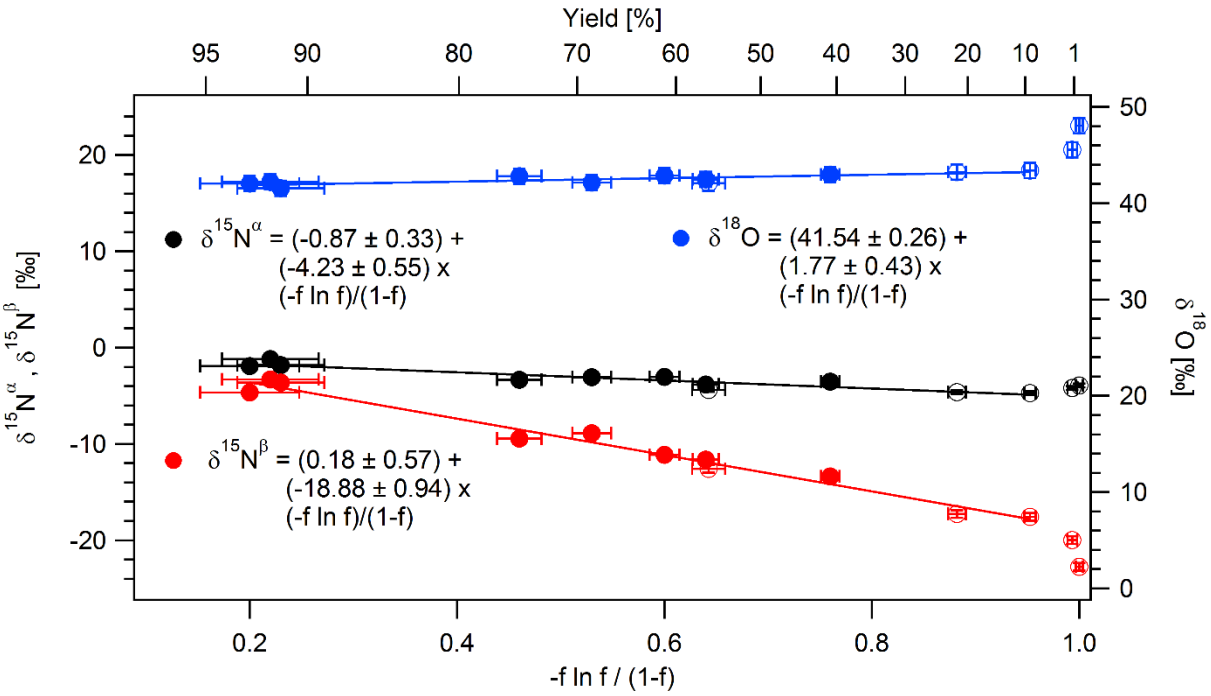

Figure 1. Site-specific isotopic composition ($\delta^{15}N^{\alpha}$, $\delta^{15}N^{\beta}$, $\delta^{18}O$) of the accumulated product gas N_2O obtained by thermal decomposition of NH_4NO_3 (P1) with different hold times (1 to 24 hours) and yields as analysed by QCLAS. Filled / open symbols represent N_2O produced by thermal decomposition in quartz glass 150 mL round bottom flasks / 6 mL ampoules, respectively. In accordance with the Rayleigh fractionation model, $\delta^{15}N^{\alpha}$, $\delta^{15}N^{\beta}$, $\delta^{18}O$ display a linear relationship versus –f ln f / (1-f), with f being the fraction of unreacted substrate and the isotope enrichment factor (ε) the slope of the regression line. Data points with a N_2O yield below 5 % were not included in the fit as they show a deviation from the linear relationship, and delta values are outside the 2 σ confidence interval of the linear regression line for $\delta^{18}O$. The displayed error bars represent the (1σ) uncertainties in yield of the NH_4NO_3 decomposition reaction (X axis) and the delta values as analysed by QCLAS (Y axis).

329 ^{15}N and ^{18}O isotope effects during NH_4NO_3 thermal decomposition was experimentally
330 determined by Friedman and Bigeleisen[12]. They observed an increase in the *m/z* 45 / 44 isotope
331 ratio of the accumulated N_2O product gas, i.e. ($^{14}N^{15}N^{16}O$+$^{15}N^{14}N^{16}O$)/$^{14}N^{14}N^{16}O$, by 7.5 ± 1
332 ‰ for extended decomposition periods, where they assumed complete reaction, in comparison
333 to one percent decomposition. For low reaction yields, i.e. high f values, –f ln f / (1-f) tends
334 towards 1 and thus Eqn. (1) can be approximated by Eqn. (2)[32]:

335 $$\delta_{N_2O} = \delta_{NH_4NO_3} + \varepsilon \quad (2)$$

336 The difference between the isotope enrichment factor determined by Friedman and
337 Bigeleisen[12] of -7.5 ± 1 ‰ and our results (-11.6 ± 0.7 ‰, calculated as the mean of $\varepsilon_{NH4\text{-}15N\beta}$
338 and $\varepsilon_{NO3\text{-}15N\alpha}$), might be partly explained by incomplete reaction, which is not considered in the
339 applied approximations. Zielinski et al.[33] interpreted results from Friedman and Bigeleisen
340 implying that the nitrogen – oxygen bond rupture in nitrate (or nitric acid) is the reaction rate
341 and isotope fractionation determining step. Consequently, they hypothesized that ^{15}N
342 fractionation (-15 ± 1 ‰) is confined to the conversion of the NO_3^- nitrogen atom to the α
343 position of the N_2O molecule. This assumption is in contrast to our experimental observations,
344 where ^{15}N fractionation was found to be substantially more pronounced for the conversion of
345 the NH_4^+ nitrogen atom to the β position of the N_2O molecule. The disparity of the two nitrogen
346 atoms can be interpreted with respect to the multi-step ionic reaction mechanism proposed for
347 the NH_4NO_3 thermal decomposition at temperatures below 563 K (see Brower et al.[34] and
348 references therein). The exact reasoning behind the observed isotope fractionation effects,
349 however, is beyond the scope of the current manuscript. In principle, ^{15}N fractionation for the
350 conversion of the ammonia nitrogen atom to the β position of the N_2O molecule might occur
351 during the initial reaction step, NH_4NO_3 dissociation into ammonia (NH_3) and nitric acid
352 (HNO_3)[35], as studied by Urey et al.[36, 37], or the oxidation of NH_3 by a nitronium ion (NO_2^+),

353 which yields N_2O and H_2O. NO_2^+ is generated in an intermediate reaction step by protonation
354 of HNO_3 to $H_2NO_3^+$ and H_2O cleavage[38].

355 Regarding the ^{18}O content in N_2O Friedman and Bigeleisen[12] observed two effects, a five per
356 mil decrease in the $^{14}N^{14}N^{18}O/^{14}N^{14}N^{16}O$ ratio of N_2O with one percent yield for the NH_4NO_3
357 decomposition reaction compared to extended reaction times, and a 23 ± 3 ‰ difference
358 between the ($^{14}N^{14}N^{18}O/^{14}N^{14}N^{16}O$) and the ($H_2{}^{18}O/H_2{}^{16}O$) ratio. The second is equivalent to a
359 15 ‰ higher ^{18}O content in N_2O compared to the NH_4NO_3 starting material. Both observations,
360 a slight decrease in the ^{18}O content with increasing N_2O yield (Figure 1) and an around 15 ‰
361 increase in the ^{18}O content of N_2O compared to NH_4NO_3 starting material (Table 1), are in
362 accordance with our results.

363 **Isotope fractionation effects during thermal decomposition of NH_4NO_3 – dynamic method**
364 Figure 2 (left) displays instantaneous site-specific isotopic composition ($\delta^{15}N^{\alpha}$, $\delta^{15}N^{\beta}$, $\delta^{18}O$)
365 and accumulated N_2O production observed during thermal decomposition of NH_4NO_3 (P1) in
366 a progressively heated quartz glass tube (1.5 K min^{-1}) under a constant flow of high-purity
367 nitrogen gas. Real-time analysis of trace gas mixing ratios by FTIR spectroscopy indicated N_2O
368 generation at temperatures above 463 K and maximum production at peak temperatures (543
369 K). In addition, release of stoichiometric amounts of the reaction by-product water vapour
370 (H_2O), and trace amounts (≤ 1 % of N_2O) of the dissociation products NH_3 and HNO_3, as well
371 as the side-product nitrogen dioxide (NO_2) were detected (data not shown). The integrated
372 overall yield of the dynamic decomposition experiment in N_2O (0.17 mmol) was only 19 % of
373 the starting material (0.9 mmol), as vaporised NH_4NO_3 reactant and dissociation product (NH_3,
374 HNO_3) were flushed out of the heated glass tube and adsorbed (or re-crystallized) at "cold
375 spots" downstream of the heated tube. This is in contrast to the static decomposition
376 experiments, where reaction yields of 91 to 93 % were achieved at maximum decomposition
377 time.

Plotting the delta values of the accumulated N_2O product as a function of –f ln f / (1-f) according to Eqn. (1) (Figure 2 (right)) indicates similar isotope enrichment factors for the dynamic decomposition experiment as compared to the static decomposition discussed in the previous section (Figure 1). This agreement is despite the fact, that a substantial fraction of the unreacted NH_4NO_3 substrate as well as the dissociation products (NH_3, HNO_3) evaded thermal decomposition by evaporation. Deviations in delta values between static and dynamic decomposition experiments might be due to fractionation effects attributed to evaporation.

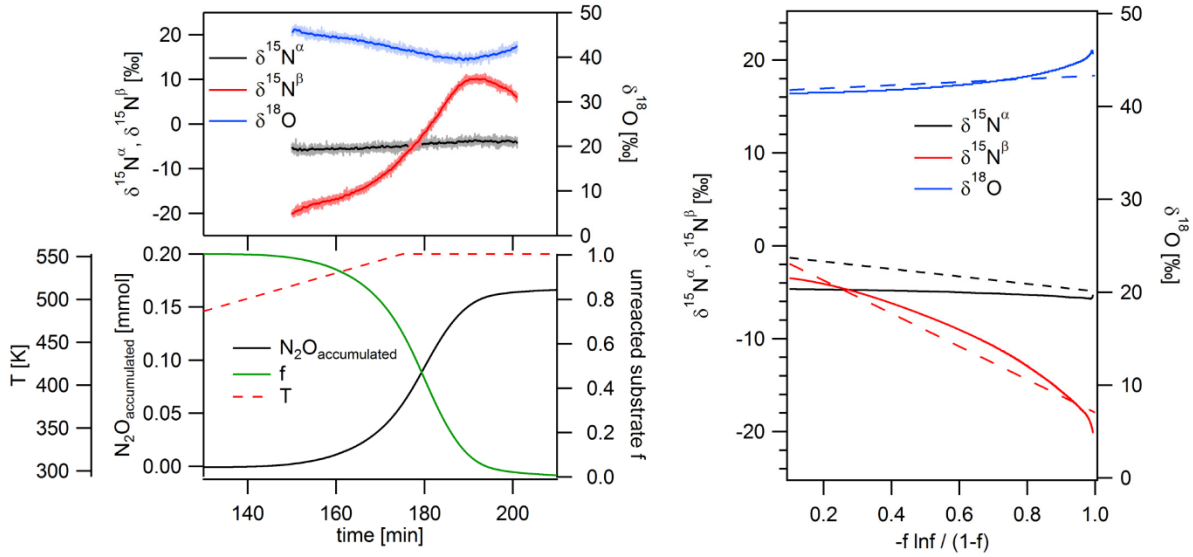

Figure 2. Thermal decomposition of NH_4NO_3 to N_2O, under a constant flow of high-purity nitrogen gas, in a progressively heated quartz glass tube (1.5 K min^{-1}). (left) Temperature of the quartz glass tube and accumulated N_2O production based on FTIR results. The fraction of unreacted substrate (f) is approximated in relation to the total N_2O yield (19 %). Changes in the site-specific isotopic composition of the N_2O product gas indicate strong isotope fractionation effects. (right) solid lines: Isotopic composition of the accumulated product N_2O derived from the dynamic decomposition experiment plotted versus -f ln f / (1-f); dotted lines: Isotopic composition of the accumulated product N_2O versus -f ln f / (1-f) as derived from the static decomposition experiments (Figure 1).

Reassessment of the NH_4NO_3 decomposition reaction

Within this section the validity of the NH_4NO_3 decomposition reaction to scale the N_2O site-specific isotopic composition relative to the international isotope ratio standard AIR-N_2 is assessed. This is accomplished by comparison of site-specific isotopic composition of the thermal decomposition product N_2O, at maximum reaction yield (90.6 ± 2.3 % to 94.4 ± 2.4 %) of the static decomposition experiments, with moiety-specific isotope analysis in the reactant NH_4NO_3 (P1 – P4, Table 1). Results in Table 1 indicate a substantial ^{15}N depletion in N_2O ($\delta^{15}N^{bulk}$) both analysed by QCLAS (Empa) as well as IRMS (MPI-BGC) as compared to the NH_4NO_3 substrate ($\delta^{15}N$-NH_4NO_3, IRMS, Lab 1 – 3) by 0.67 ± 0.43 ‰ or 1.14 ± 0.37 ‰, respectively. This might be either caused by the generation of reaction side-products (e.g. N_2) with higher ^{15}N content, ^{15}N fractionation during thermal NH_4NO_3 decomposition as described in the previous sections, or a combination of both. The yield of volatile reaction side-products, noncondensable at liquid nitrogen temperatures and hypothesised to be mainly N_2, in our static decomposition experiments was around 4 %. To compensate for N_2 production Toyoda et al.[3] analysed $\delta^{15}N$-N_2 and used differences between $\delta^{15}N$-NH_4NO_3 and $\delta^{15}N$-N_2 to correct $\delta^{15}N^{bulk}$ (N_2O) by -0.1 to -0.9 ‰, thus in a similar range than observed in this study. In contrast, Westley et al.[14] used a constant offset correction by -0.79 ‰ irrespective of the observed $\delta^{15}N$-N_2 values and the reaction yield. Differences in $\delta^{15}N^{bulk}$ (N_2O) between IRMS (MPI-BGC) and QCLAS (Empa) by 0.46 ± 0.13 ‰, were probably caused by differences in the anchoring of the analytical results. This observation also confirms earlier findings by Mohn et al. (0.39 ‰)[7] and Toyoda et al (0.3 ‰)[3], where discrepancies in $\delta^{15}N^{bulk}$ of N_2O were attributed to isotope fractionation during incomplete NH_4NO_3 decomposition.

Differences between the N_2O site-specific isotopic composition and the moiety-specific isotopic composition of the NH_4NO_3 salts, thus between $\delta^{15}N^{\alpha}$ versus $\delta^{15}N\text{-}NO_3^-$ and $\delta^{15}N^{\beta}$ versus $\delta^{15}N\text{-}NH_4^+$, display a similar magnitude -0.72 ± 0.21 ‰ and -0.61 ± 0.80 ‰, respectively (Table 1). Consequently, the N_2O site-preference, defined as the difference between $\delta^{15}N^{\alpha}$ and $\delta^{15}N^{\beta}$, measured by QCLAS, and the difference in $\delta^{15}N\text{-}NO_3^-$ - $\delta^{15}N\text{-}NH_4^+$, as analysed by IRMS, agreed within 0.10 ± 0.80 ‰ (-0.9 to 1.1 ‰). Therefore, in summary, it can be concluded that the results of the NH_4NO_3 thermal decomposition technique, developed by Toyoda and Yoshida[3] to calibrate N_2O site preference, can be reproduced. This was already confirmed by Marian Westley et al.[14], but the explanatory power of their experiments was limited, due to a much lower reaction yield of only 55 to 74 %, which may have affected the isotopic composition of the decomposition product N_2O. The accuracy of the NH_4NO_3 thermal decomposition reaction to link the N_2O SP to the international isotope ratio scales, however, is restricted by significant formation of side-products (e.g. N_2) in combination with the observed site-specific isotope fractionation effects. The formation of side-products also prevents the use of the Rayleigh model to correct fractionation effects by incomplete reaction.

The validity of the NH_4NO_3 decomposition reaction to link the ^{15}N site preference of N_2O to the international isotope ratio scale AIR-N_2 could be enhanced by a further increase in the reaction yield. The yield of the NH_4NO_3 decomposition reaction and the product distribution, however, depends on various factors such as sample size and purity, presence of other chemicals (catalysts) as well as the reaction conditions, e.g. pressure, temperature and heating rate[39]. Sulfuric and hydrochloric acid were both shown to catalyse the NH_4NO_3 decomposition reaction[40], the mechanism for both acids, however, is different. Sulfuric acid replaces the nitrate ion in the NH_4NO_3 molecule, promoting the build-up of HNO_3, while hydrochloric acid increases the generation of the intermediate product $NH_3NO_2^+$[41]. But, the addition of chlorides may lead to enhanced production of the side-product N_2 by decomposition of the reaction

444 intermediate NH_2Cl[41]. Similarly, addition of Cr^{3+} catalyses NH_4NO_3 thermal decomposition
445 favouring the exothermic formation of N_2[42], which prevents using this technique for
446 standardisation of ^{15}N site preference in N_2O. A promising technique might be the
447 decomposition of NH_4NO_3 in a NH_4HSO_4 – $(NH_4)_2SO_4$ melt was shown to yield 99 – 99.5 %
448 N_2O and only 1.0 – 0.5 % N_2[43] offering the potential to link the ^{15}N isotopic composition of
449 the central (α) N atom of the N_2O molecule via analysis of $\delta^{15}N\text{-}NO_3^-$ to the international
450 isotope ratio scales.

451 Although it is not in the main focus of the presented study it is worth mentioning the observed
452 differences in $\delta^{18}O$ analysed by QCLAS (Empa) and IRMS (MPI-BGC) (Table 1). Differences
453 were only 0.31 ‰ for P4 but 1.40 ± 0.25 ‰ (1.19 to 1.74 ‰) for the samples P1 – P3 and might
454 be rationalized by differences in the referencing to the international isotope ratio scale, in
455 particular an expanded uncertainty of QCLAS measurements for $\delta^{18}O$ induced by the
456 implemented calibration strategy (Table 1). The high uncertainty in $\delta^{18}O$ values analysed by
457 QCLAS was provoked by the limited range in $\delta^{18}O$ values covered by the standards (CG1-1,
458 CG1-2 versus CG2) relative to the measured delta values especially for P1 – P3.

459

460

Table 1. Isotopic composition of NH_4NO_3 reactant P1 – P4 (IRMS Lab 1 – 3) and the thermal decomposition product N_2O by IRMS for $\delta^{15}N^{bulk}$ and $\delta^{18}O$ values and QCLAS for $\delta^{15}N^{\alpha}$, $\delta^{15}N^{\beta}$ and $\delta^{18}O$ values, given in δ-units. IRMS and QCLAS analysis was performed versus the international isotope ratio scales AIR-N_2 ($^{15}N/^{14}N$) and VSMOW ($^{18}O/^{16}O$). QCLAS analysis is based on calibration gases analysed at Tokyo Institute of Technology, using their analytical technique as a link to the international scales. The indicated uncertainty for IRMS and QCLAS results was calculated as described in the experimental section.

			P1	P2	P3	P4	n
Lab 1	NH_4NO_3	$\delta^{15}N\text{-}NO_3^-$	-0.7 ± 0.1	17.4 ± 0.02	36.7 ± 0.02	-35.5 ± 0.2	4
Lab 2			-0.7 ± 0.1	17.0 ± 0.2	36.1 ± 0.1	-35.3 ± 0.1	5
Lab 3			-1.1 ± 0.1	16.9 ± 0.2	36.1 ± 0.3	-35.7 ± 0.2	3-4
Average			-0.8 ± 0.2	17.1 ± 0.2	36.3 ± 0.3	-35.5 ± 0.2	
QCLAS	N_2O	$\delta^{15}N^{\alpha}$	-1.8 ± 0.2	16.3 ± 0.2	35.8 ± 0.4	-36.1 ± 0.4	3
IRMS			-	-	-	-	-
Lab 1	NH_4NO_3	$\delta^{15}N\text{-}NH_4^+$ [a]	-4.1 ± 0.1	-5.7 ± 0.1	62.4 ± 0.3	-51.9 ± 0.3	[a]
Lab 2			-3.7 ± 0.2	-4.8 ± 0.2	63.0 ± 0.2	-51.5 ± 0.2	[a]
Lab 3			-2.8 ± 0.2	-2.3 ± 0.2	64.0 ± 0.3	-50.2 ± 0.2	[a]
Average			-3.5 ± 0.6	-4.3 ± 1.4	63.1 ± 0.7	-51.2 ± 0.7	
QCLAS	N_2O	$\delta^{15}N^{\beta}$	-3.8 ± 0.4	-5.2 ± 0.4	63.5 ± 1.0	-52.9 ± 0.6	3
IRMS			-	-	-		-
Lab 1	NH_4NO_3	$\delta^{15}N\text{-}NO_3^- - \delta^{15}N\text{-}NH_4$	3.3 ± 0.1	23.1 ± 0.1	-25.7 ± 0.3	16.4 ± 0.4	[b]
Lab 2			3.0 ± 0.2	21.8 ± 0.4	-26.9 ± 0.3	16.2 ± 0.2	[b]
Lab 3			1.7 ± 0.5	19.2 ± 0.3	-27.9 ± 0.5	14.5 ± 0.3	[b]
Average			2.7 ± 0.7	21.4 ± 1.6	-26.8 ± 0.9	15.7 ± 0.8	
QCLAS	N_2O	SP	1.9 ± 0.4	21.4 ± 0.4	-27.7 ± 1.0	16.8 ± 0.8	3
IRMS			-	-	-	-	-
Lab 1	NH_4NO_3	$\delta^{15}N$	-2.4 ± 0.1	5.8 ± 0.1	49.5 ± 0.3	-43.7 ± 0.2	4
Lab 2			-2.2 ± 0.1	6.1 ± 0.1	49.5 ± 0.1	-43.4 ± 0.1	5
Lab 3			-1.9 ± 0.2	7.3 ± 0.1	50.0 ± 0.1	-43.0 ± 0.1	3-4
Average			-2.2 ± 0.2	6.4 ± 0.6	49.7 ± 0.2	-43.4 ± 0.3	
QCLAS	N_2O	$\delta^{15}N^{bulk}$	-2.8 ± 0.2	5.5 ± 0.2	49.7 ± 0.5	-44.5 ± 0.4	3
IRMS			-3.2 ± 0.01	5.2 ± 0.01	49.1 ± 0.01	-45.0 ± 0.003	3
Lab 1	NH_4NO_3	$\delta^{18}O$	28.0 ± 0.3	27.4 ± 0.3	27.5 ± 0.1	18.4 ± 0.3	4
Lab 2			-	-	-	-	[c]
Lab 3			-	-	-	-	[c]
Average			28.0	27.4	27.5	18.4	
QCLAS	N_2O	$\delta^{18}O$	41.6 ± 0.8	41.8 ± 0.8	42.2 ± 0.8	33.6 ± 0.5	3
IRMS			42.8 ± 0.01	43.0 ± 0.003	43.9 ± 0.03	33.9 ± 0.02	3

[a] calculated from: $\delta^{15}N\text{-}NH_4^+ = 2 \times \delta^{15}N\text{-}NH_4NO_3 - \delta^{15}N\text{-}NO_3^-$

[b] calculated from: $\delta^{15}N\text{-}NH_4^+ - \delta^{15}N\text{-}NO_3^-$

[c] not analysed

CONCLUSION

The study investigates the validity of the NH_4NO_3 decomposition technique to link NH_4^+ and NO_3^- moiety-specific $\delta^{15}N$ analysis by IRMS to N_2O site-specific nitrogen isotopic composition. It confirms that the moiety-specific nitrogen isotopic composition is transferred from the NH_4NO_3 starting material to the N_2O product gas. The accuracy of this approach for calibration of $\delta^{15}N^{\alpha}$ and $\delta^{15}N^{\beta}$, however, was found to be limited by non-quantitative NH_4NO_3 decomposition in combination with substantially different isotope enrichment factors for the conversion of the NO_3^- or NH_4^+ nitrogen atom to the α or β position of the N_2O molecule and generation of side-product (e.g. N_2). Thereby, the study reveals that the accuracy of the NH_4NO_3 decomposition reaction currently confines the anchoring of N_2O site specific isotopic composition to the international isotope ratio scale AIR-N_2. To improve inter-laboratory compatibility for N_2O isotopomers analysis, the authors suggest to establish a set of N_2O isotope reference materials with appropriate site-specific isotopic composition in the form of community standards.

ACKNOWLEDGEMENTS

The study was supported by the European Metrology Research Programme (EMRP) ENV52 project 'Metrology for high-impact greenhouse gases'. The EMRP is jointly funded by the EMRP participating countries within EURAMET and the European Union. In addition, instrumental developments at EMPA were funded by the Swiss National Science Foundation (SNSF) within project 200021L_150237.

REFERENCES

[1] C. Decock, J. Six. How reliable is the intramolecular distribution of ^{15}N in N_2O to source partition N_2O emitted from soil? *Soil Biol. Biochem.* **2013**, *65*, 114.

[2] S. Toyoda, N. Yoshida, K. Koba. Isotopocule analysis of biologically produced nitrous oxide in various environments. *Mass Spectrom. Rev.* **2015**, DOI: 10.1002/mas.21459.

[3] S. Toyoda, N. Yoshida. Determination of nitrogen isotopomers of nitrous oxide on a modified isotope ratio mass spectrometer. *Anal. Chem.* **1999**, *71*, 4711.

[4] C. A. M. Brenninkmeijer, T. Röckmann. Mass spectrometry of the intramolecular nitrogen isotope distribution of environmental nitrous oxide using fragment-ion analysis. *Rapid Commun. Mass Spectrom.* **1999**, *13*, 2028.

[5] H. Wächter, J. Mohn, B. Tuzson, L. Emmenegger, M. W. Sigrist. Determination of N_2O isotopomers with quantum cascade laser based absorption spectroscopy. *Opt. Express* **2008**, *16*, 9239.

[6] J. Heil, B. Wolf, N. Brueggemann, L. Emmenegger, B. Tuzson, H. Vereecken, J. Mohn. Site-specific ^{15}N isotopic signatures of abiotically produced N_2O. *Geochim. Cosmochim. Acta* **2014**, *139*, 72.

[7] J. Mohn, B. Tuzson, A. Manninen, N. Yoshida, S. Toyoda, W. A. Brand, L. Emmenegger. Site selective real-time measurements of atmospheric N_2O isotopomers by laser spectroscopy. *Atmos. Meas. Tech.* **2012**, *5*, 1601.

[8] B. Wolf, L. Merbold, C. Decock, B. Tuzson, E. Harris, J. Six, L. Emmenegger, J. Mohn. First on-line isotopic characterization of N_2O above intensively managed grassland. *Biogeosciences* **2015**, *12*, 2517.

[9] D. V. Erler, T. M. Duncan, R. Murray, D. T. Maher, I. R. Santos, J. R. Gatland, P. Mangion, B. D. Eyre. Applying cavity ring-down spectroscopy for the measurement of dissolved nitrous oxide concentrations and bulk nitrogen isotopic composition in aquatic systems: Correcting for interferences and field application. *Limnol. Oceanogr. Methods* **2015**, *13*, 391.

[10] T. B. Coplen. Guidelines and recommended terms for expression of stable-isotope-ratio and gas-ratio measurement results. *Rapid Commun. Mass Spectrom.* **2011**, *25*, 2538.

[11] J. Mohn, B. Wolf, S. Toyoda, C. T. Lin, M. C. Liang, N. Brüggemann, H. Wissel, A. E. Steiker, J. Dyckmans, L. Szwec, N. E. Ostrom, K. L. Casciotti, M. Forbes, A. Giesemann, R. Well, R. R. Doucett, C. T. Yarnes, A. R. Ridley, J. Kaiser, N. Yoshida. Interlaboratory assessment of nitrous oxide isotopomer analysis by isotope ratio mass spectrometry and laser spectroscopy: Current status and perspectives. *Rapid Commun. Mass Spectrom.* **2014**, *28*, 1995.

[12] L. Friedman, J. Bigeleisen. Oxygen and nitrogen isotope effects in the decomposition of ammonium nitrate. *J. Chem. Phys.* **1950**, *18*, 1325.

[13] J. Kaiser, S. Park, K. A. Boering, C. A. M. Brenninkmeijer, A. Hilkert, T. Röckmann. Mass spectrometric method for the absolute calibration of the intramolecular nitrogen isotope distribution in nitrous oxide. *Anal. Bioanal. Chem.* **2004**, *378*, 256.

[14] M. B. Westley, B. N. Popp, T. M. Rust. The calibration of the intramolecular nitrogen isotope distribution in nitrous oxide measured by isotope ratio mass spectrometry. *Rapid Commun. Mass Spectrom.* **2007**, *21*, 391.

[15] D. W. T. Griffith, S. D. Parkes, V. Haverd, C. Paton-Walsh, S. R. Wilson. Absolute calibration of the intramolecular site preference of ^{15}N fractionation in tropospheric N_2O by FT-IR spectroscopy. *Anal. Chem.* **2009**, *81*, 2227.

[16] K. L. Casciotti, D. M. Sigman, M. G. Hastings, J. K. Böhlke, A. Hilkert. Measurement of the oxygen isotopic composition of nitrate in seawater and freshwater using the denitrifier method. *Anal. Chem.* **2002**, *74*, 4905.
[17] D. M. Sigman, K. L. Casciotti, M. Andreani, C. Barford, M. Galanter, J. K. Böhlke. A bacterial method for the nitrogen isotopic analysis of nitrate in seawater and freshwater. *Anal. Chem.* **2001**, *73*, 4145.
[18] P. D. Brooks, H. Geilmann, R. A. Werner, W. A. Brand. Improved precision of coupled $\delta^{13}C$ and $\delta^{15}N$ measurements from single samples using an elemental analyzer/isotope ratio mass spectrometer combination with a post-column six-port valve and selective CO_2 trapping; improved halide robustness of the combustion reactor using CeO_2. *Rapid Commun. Mass Spectrom.* **2003**, *17*, 1924.
[19] R. A. Werner, B. A. Bruch, W. A. Brand. ConFlo III - An interface for high precision $\delta^{13}C$ and $\delta^{15}N$ analysis with an extended dynamic range. *Rapid Commun. Mass Spectrom.* **1999**, *13*, 1237.
[20] R. A. Werner, W. A. Brand. Referencing strategies and techniques in stable isotope ratio analysis. *Rapid Commun. Mass Spectrom.* **2001**, *15*, 501.
[21] K. L. Casciotti, J. K. Böhlke, M. R. McIlvin, S. J. Mroczkowski, J. E. Hannon. Oxygen isotopes in nitrite: Analysis, calibration, and equilibration. *Anal. Chem.* **2007**, *79*, 2427.
[22] M. R. McIlvin, K. L. Casciotti. Technical updates to the bacterial method for nitrate isotopic analyses. *Anal. Chem.* **2011**, *83*, 1850.
[23] M. R. McIlvin, K. L. Casciotti. Fully automated system for stable isotopic analyses of dissolved nitrous oxide at natural abundance levels. *Limnol. Oceanogr. Methods* **2010**, *8*, 54.
[24] P. Schleppi, I. Bucher-Wallin, M. Saurer, M. Jäggi, W. Landolt. Citric acid traps to replace sulphuric acid in the ammonia diffusion of dilute water samples for ^{15}N analysis. *Rapid Commun. Mass Spectrom.* **2006**, *20*, 629.
[25] J. Mohn, A. M. Forss, S. Brühlmann, K. Zeyer, R. Lüscher, L. Emmenegger, P. Novak, N. Heeb. Time-resolved ammonia measurement in vehicle exhaust. *Int. J. Environ. Pollut.* **2004**, *22*, 342.
[26] J. Mohn, M. J. Zeeman, R. A. Werner, W. Eugster, L. Emmenegger. Continuous field measurements of $\delta^{13}C$-CO_2 and trace gases by FTIR spectroscopy. *Isot. Environ. Health Stud.* **2008**, *44*, 241.
[27] J. R. Köster, R. Well, B. Tuzson, R. Bol, K. Dittert, A. Giesemann, L. Emmenegger, A. Manninen, L. Cárdenas, J. Mohn. Novel laser spectroscopic technique for continuous analysis of N_2O isotopomers - Application and intercomparison with isotope ratio mass spectrometry. *Rapid Commun. Mass Spectrom.* **2013**, *27*, 216.
[28] E. Harris, A. Joss, L. Emmenegger, M. Kipf, B. Wolf, J. Mohn, P. Wunderlin. Isotopic evidence for nitrous oxide production pathways in a partial nitritation-anammox reactor. *Water Res.* **2015**, *83*, 258.
[29] E. Harris, K. Zeyer, R. Kegel, B. Müller, L. Emmenegger, J. Mohn. Nitrous oxide and methane emissions and nitrous oxide isotopic composition from waste incineration in Switzerland. *Waste Manage.* **2015**, *35*, 135.
[30] P. Werle, R. Mucke, F. Slemr. The limits of signal averaging in atmospheric trace-gas monitoring by tunable diode-laser absorption-spectroscopy (TDLAS). *Appl. Phys.* **1993**, *57*, 131.
[31] E. Barkan, B. Luz. High precision measurements of $^{17}O/^{16}O$ and $^{18}O/^{16}O$ ratios in H_2O. *Rapid Commun. Mass Spectrom.* **2005**, *19*, 3737.
[32] A. Mariotti, J. C. Germon, P. Hubert, P. Kaiser, R. Letolle, A. Tardieux, P. Tardieux. Experimental determination of nitrogen kinetic isotope fractionation: Some principles; illustration for the denitrification and nitrification processes. *Plant Soil* **1981**, *62*, 413.

[33] M. Zielinski, A. Zielinska, H. Papiernik-Zielinska. Comments on the isotopic and chemical studies of the thermal decomposition of ammonium nitrate. *Pol. J. Chem.* **2002**, *76*, 1519.
[34] K. R. Brower, J. C. Oxley, M. Tewari. Evidence for homolytic decomposition of ammonium nitrate at high temperature. *J. Phys. Chem.* **1989**, *93*, 4029.
[35] W. M. Chien, D. Chandra, K. H. Lau, D. L. Hildenbrand, A. M. Helmy. The vaporization of NH_4NO_3. *J. Chem. Thermodyn.* **2010**, *42*, 846.
[36] H. G. Thode, H. C. Urey. The further concentration of N^{15}. *J. Chem. Phys.* **1939**, *7*, 34.
[37] H. C. Urey, J. R. Huffman, H. G. Thode, M. Fox. Concentration of N^{15} by chemical methods. *J. Chem. Phys.* **1937**, *5*, 856.
[38] J. W. Chapman, A. N. Strachan. The rate of nitronium ion formation from nitric acid in aqueous sulphuric acid. *Chem. Commun.* **1974**, 293.
[39] S. Chaturvedi, P. N. Dave. Review on thermal decomposition of ammonium nitrate. *J. Energ. Mater.* **2013**, *31*, 1.
[40] J. Sun, Z. Sun, Q. Wang, H. Ding, T. Wang, C. Jiang. Catalytic effects of inorganic acids on the decomposition of ammonium nitrate. *J. Hazard. Mater.* **2005**, *127*, 204.
[41] J. H. MacNeil, H. T. Zhang, P. Berseth, W. C. Trogler. Catalytic decomposition of ammonium nitrate in superheated aqueous solutions. *J. Am. Chem. Soc.* **1997**, *119*, 9738.
[42] S. Skaribas, T. C. Vaimakis, P. J. Pomonis. Threshold limits and kinetics of the non-isothermal decomposition of ammonium nitrate catalysed by chromium ions. *Thermochim. Acta* **1990**, *158*, 235.
[43] Z. G. Szabó, E. Hollós, J. Trompler. Thermal decomposition of ammonium nitrate without side-reactions. *Z. Phys. Chem.* **1985**, *144*, 187.